Electronic Supplementary Material (ESI) for New Journal of Chemistry.

Supporting Information Section

Supramolecular Kinetic Effects by Pillararenes: The Synergism Between Spatiotemporal and Preorganization Concepts in Decarboxylation Reactions

Eduardo V. Silveira,[a],* Rodrigo Montecinos,[b] Leandro Scorsin,[a] Luis Garcia-Rio,[c],* Michelle Medeiros,[a] Vanessa Nascimento,[d] Faruk Nome,[a],† Ricardo F. Affeldt,[a] and Gustavo A. Micke,[a]

[a]*Department of Chemistry, Federal University of Santa Catarina, Florianópolis – SC, 88040-900, Brazil.*
[b]*Faculdad de Química, Pontificia Universidad Católica de Chile, Av. Vicuña Mackenna 4860, Santiago, Chile.*
[c]*Departamento de Química Física, Centro de Investigación en Química Biolóxica e Materiais Moleculares (CIQUS), Universidade de Santiago de Compostela, 15782 Santiago de Compostela, Spain.*
[d]*Department of Organic Chemistry, Fluminense Federal University, Niterói – RJ, 24020-150, Brazil.*

Section

1. Synthetic Procedures

The CBI derivatives and pillararenes were prepared on the basis of the literature,[1,2] with the modifications detailed below.

Syntheses of P5A and P6A. Scheme S1 shows the three reaction steps used to obtain the P5A and P6A: (step 1) bromination of hydroquinone, (step 2) cyclization promoted by Lewis acid and (step 3) functionalization with trimethylammonium groups. All reaction steps are detailed below.

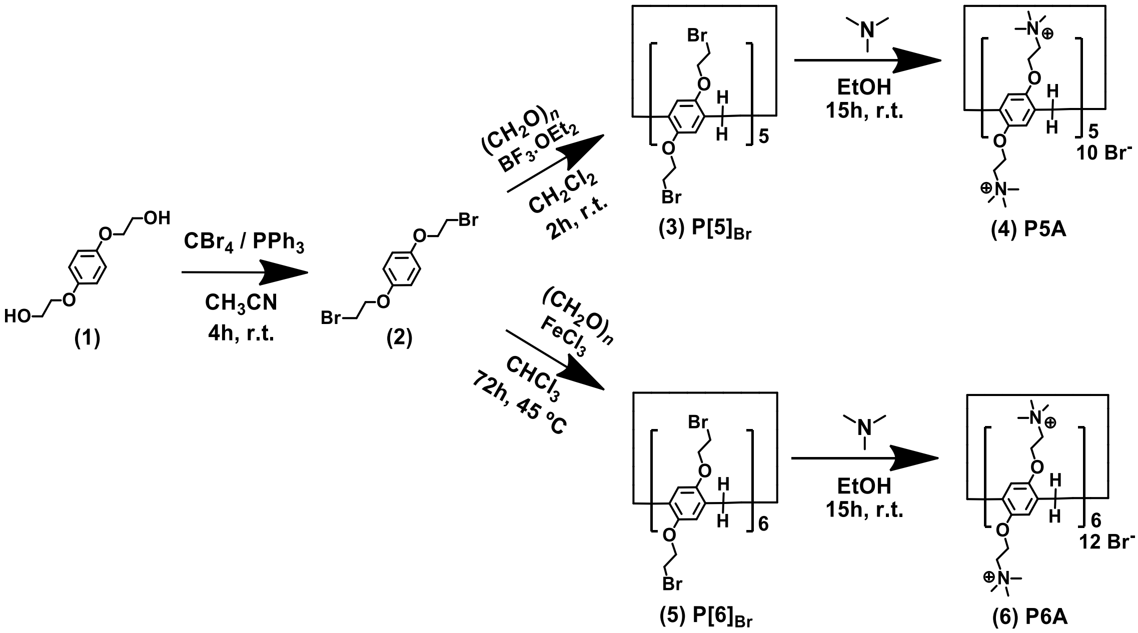

Scheme S1. Synthetic routes used to obtain P5A (**4**) and P6A (**6**).

(Step 1) In a reaction flask under argon atmosphere hydroquinone (10.0 mmol), triphenylphosphine (23.81 mmol) and dry acetonitrile (50.0 mL) were added. This reaction mixture was cooled to 0 °C and the carbon tetrabromide (23.81 mmol) was slowly added. The reaction mixture was stirred at room temperature for 4 h. After this period, cold water (40.0 mL) was added, resulting in a white precipitate. The precipitate was collected, washed with MeOH/H_2O (3:2, 3 × 25.0 mL), recrystallized from methanol and dried under vacuum. Yield 93 % of the compound **2** as a white solid. ^{1}H NMR (200 MHz, $CDCl_3$, TMS) δ (ppm): 6.86 (s, 4H); 4.24 (t, 4H, J = 4 Hz); 3.61 (t, 4H, J = 4 Hz). ^{13}C{^{1}H} NMR (50 MHz, $CDCl_3$, residual solvent as reference) δ (ppm): 152.9; 116.2; 68.8; 29.4.

(Step 2, for P5A) In a solution of brominated hydroquinone in CH_2Cl_2 (230 mL), paraformaldehyde (30.87 mmol) and boron trifluoride diethyl etherate (33.86 mmol) were added under argon atmosphere. The resulting mixture was stirred during 2 h at room temperature. After this time, the reaction mixture was washed with water, saturated sodium bicarbonate solution and brine. The organic layer was dried over $MgSO_4$ and the solvent was removed by vacuum. The residue was purified by column chromatography (CH_2Cl_2:hexane) yielding 70 % of the brominated pillar[5]arene (compound **3**) as a white solid. ^1H NMR (200 MHz, $CDCl_3$, TMS) δ (ppm): 6.91 (s, 10H); 4.23 (t, 20H, J = 4 Hz); 3.84 (s, 10H); 3.63 (t, 20H, J = 4 Hz). $^{13}C\{^1H\}$ NMR (50 MHz, $CDCl_3$, residual solvent as reference) δ (ppm): 149.8; 129.2; 116.2; 69.1; 30.9; 29.5.

(Step 2, for P6A) In a solution of brominated hydroquinone in $CHCl_3$ (90 mL), paraformaldehyde (30.87 mmol) and $FeCl_3$ (1.24 mmol) were added under argon atmosphere. The resulting mixture was stirred during 72 h at 45 °C. After this time, the reaction mixture was washed with water, saturated sodium bicarbonate solution and brine. The organic layer was dried over $MgSO_4$ and the solvent was removed by vacuum. The residue was purified by column chromatography (CH_2Cl_2:hexane) yielding 30 % of the brominated pillar[6]arene (compound **5**) as a pale yellow solid. ^1H and $^{13}C\{^1H\}$ NMR chemical shifts similar to brominated pillar[5]arene.

(Step 3) In a solution of brominated pillararene (1.19 mmol) in ethanol (100.0 mL) was added trimethylamine (48.11 mmol). The reaction mixture was refluxed overnight. After this time, the precipitate was collected, washed with EtOH and dried under vacuum. Yield 95 % to P5A (white solid) and 91 % to P6A (pale yellow solid). ^1H NMR (500 MHz, D_2O, TMSP) δ (ppm): 6.86 (s, 1H), 4.37 (s, 2H), 3.85 (s, 1H), 3.72 (s, 2H), 3.14 (s, 9H). $^{13}C\{^1H\}$ NMR (126 MHz, D_2O, TMSP) δ(ppm): 149.4, 130.0, 116.5, 65.0, 63.5, 54.1, 29.5. HRMS/ESI-TOF (m/z) for P5A: $[P5A–3Br^-]^{3+}$ ($C_{85}H_{150}N_{10}O_{10}Br_7$), calculated 677.1917, found 677.1919; $[P5A–2Br^-]^{2+}$ ($C_{85}H_{150}N_{10}O_{10}Br_8$), calculated 1055.7472, found 1055.7473. HRMS/ESI-TOF (m/z) for P6A: $[P6A–3Br^-]^{3+}$ ($C_{102}H_{180}N_{12}O_{12}Br_9$), calculated 828.5472, found 828.5474; $[P6A–2Br^-]^{2+}$ ($C_{102}H_{180}N_{12}O_{12}Br_{10}$), calculated 1282.7799, found 1282.7795.

Syntheses of 6-NitroCBI and 5,6-DinitroCBI. Scheme S2 shows the five reaction steps for 6-NitroCBI and 5,6-DinitroCBI syntheses: (step 1) esterification of 2,4-dinitrophenylacetic acid, (step 2) cyclization of isoxazole ring, (step 3) acidic hydrolysis of ester to form 6-NitroCBI, (step 4) nitration in 5-position of 1,2-benzisoxazole and (step 5) acidic hydrolysis of ester to form 5,6-DinitroCBI. All reaction steps are detailed below.

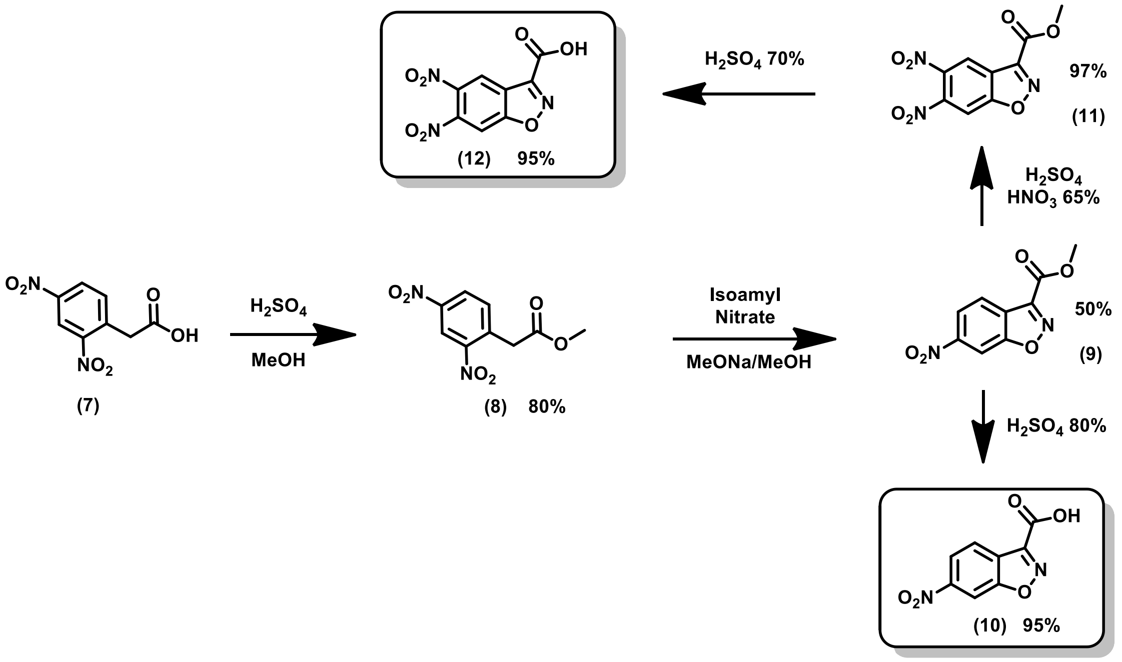

Scheme S2. Synthetic routes used to obtain 6-NitroCBI (**10**) and 5,6-DinitroCBI (**12**).

(Step 1) In a reaction flask under argon atmosphere, was added 2,4-dinitrophenylacetic acid **(7)** (44 mmol), methanol (5.3 mL), CH_2Cl_2 (13.0 mL) and H_2SO_4 (0.66 mL). The solution was refluxed for 20 h. After cooling, the reaction mixture was washed with 20 mL of water, 20 mL of saturated $NaHCO_3$ solution followed by 20 mL of water. The organic layer was dried over $MgSO_4$ and the solvent was removed by vaccum. After washing with ethanol the desired product (compound **8**) was obtained as a yellow oil in 80 % yield. The product was confirmed by GC-MS and used for the next step without any additional purification.

(Step 2) In a 3-neck flask equipped with reflux condenser and addition funnel was added **(8)** (14.6 mmol) and dry methanol (50 mL) at 40 ºC. Then the isoamyl nitrate (18.0 mmol) was added. In the addition funnel was added dry methanol (10.0 mL) and metallic sodium (0.330 g) and after the solid has been consumed the resulting solution was added slowly under vigorous stirring. The mixture obtained was stirred for further 4

h. After this time the suspension was cooled to room temperature and the solid was filtered off by vacuum. The yellow crystals were recrystallized with methanol. The product (compound **9**) was obtained as a yellow solid in 50 % yield. The product was confirmed by GC-MS and used for the next step without any additional purification.

(Step 3) In a reaction flask was added **(9)** (4.5 mmol) and H_2SO_4 80 % (20.0 mL). The obtained solution was stirring for 40 min at 80 ºC. After this time the reaction mixture was cooled and poured into ice. The solid formed was filtered off under vacuum and washed with cold water. Yield 95 % of the 6-NitroCBI as a white solid. ^1H NMR (200 MHz, Acetone-D_6) δ (ppm): 8.73 (s, 1H); 8.39 (s, 2H); 9.15 (s, OH). $^{13}C\{^1H\}$ NMR (50 MHz, CD_3CN:DCl 6M 1:1): 163.04; 160.46; 151.31; 149.39; 124.51; 124.15; 120.35 and 106.58.

(Step 4) In a reaction flask was added **(9)** (5.0 g) and H_2SO_4 (25.0 mL). The reaction was heated to 30 ºC and nitric acid 65 % (5.0 mL) was added under stirring. Subsequently the reaction was warmed to 50 ºC and maintained under stirring for further 4 h. Then the mixture was cooled and poured into ice. The precipitate was collected, washed with cold water and dried in a high vacuum pump. Yield 97 % of the compound **11** as a white solid. ^1H NMR (200 MHz, $CDCl_3$) δ (ppm): 8.83 (s, 1H); 8.23 (s, 1H); 4.17 (s, 3H).

(Step 5) In a reaction flask was mixed previously prepared compound **(11)** (2.0 g) and H_2SO_4 70 % (20.0 mL). The reaction was warmed to 80 ºC and stirred for 3 h. After this time the solution was cooled and poured into ice. The precipitate was collected, washed with cold water and dried in a high vacuum pump. Yield 95 % of the 5,6-DinitroCBI as a gray solid. ^1H NMR (200 MHz, Acetone-D_6) δ (ppm): 8.87 (s, 1H); 8.56 (s, 1H); 9.92 (s, OH).

2. HRMS Fragmentograms

The HRMS fragmentograms of pillararenes were recorded by using a Bruker Daltonics – micrOTOF-Q II/ESI-Qq-TOF mass spectrometer.

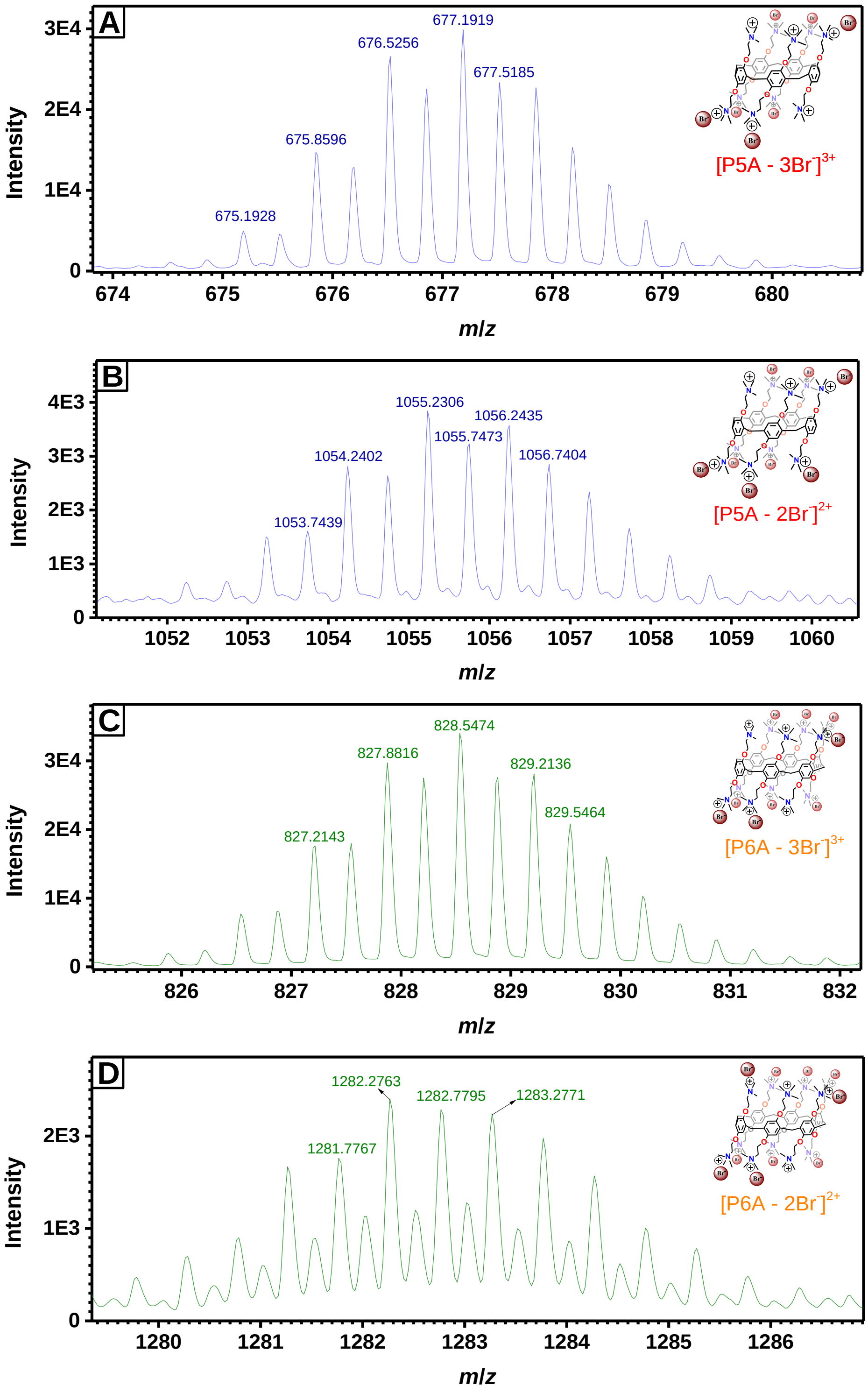

Figure S1. HRMS/ESI-TOF fragmentograms of aqueous solutions of P5A (**A** and **B**) and P6A (**C** and **D**) in positive ion mode.

3. Product Characterization and Molar Absorption Coefficients

3.1 Product characterization

The products of the decarboxylation reaction of 6-NitroCBI and 5,6-DinitroCBI (6-NitroCP and 5,6-DinitroCP, respectively) were characterized by NMR and ESI-MS experiments (Table S1 and Figures S2-S4).

Table S1. *m/z*, ^{1}H and ^{13}C{^{1}H} NMR chemical shifts of the cyanophenols (CPs) (Acetone-D$_6$; 25.0 ºC; 200 MHz; TMS).

Product	***m/z***	**NMR (δ, ppm)**	
		^{1}H	**^{13}C{^{1}H}***
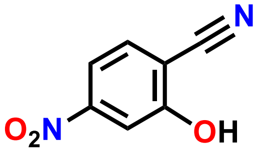 **6-NitroCP**	163.0 [CP – H^{+}]$^{–}$	δ 5.61 (s, 1H, OH); δ 8.40 (s, 2H, Ar); δ 8.74 (s, 1H, Ar);	δ 107.25; δ 120.98; δ 125.34; δ 150.38; δ 151.99; δ 160.41; δ 164.03;
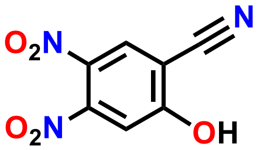 **5,6-DinitroCP**	207.8 [CP – H^{+}]$^{–}$	---- (s, 1H, OH);** δ 7.65 (s, 1H, Ar); δ 8.65 (s, 1H, Ar);	δ 104.02; δ 113.06; δ 114.06; δ 125.71; δ 133.14; δ 148.32; δ 166.11;

*Residual solvent as reference; **Exchanged with HDO (see NMR spectrum below).

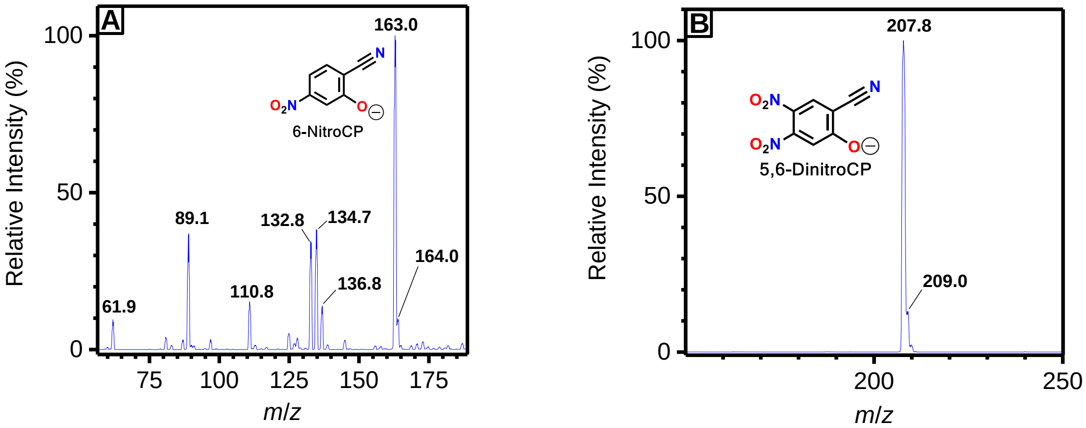

Figure S2. ESI-MS spectra of the 6-NitroCP (**A**) and 5,6-DinitroCP (**B**).

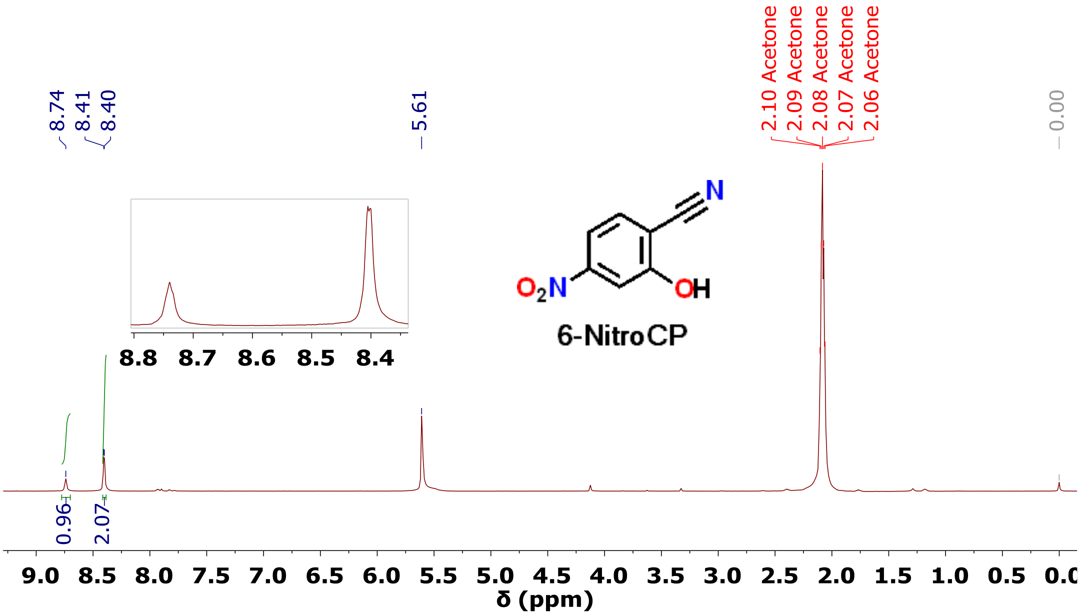

Figure S3-a. ^{1}H NMR spectra of 6-NitroCP (Acetone-D_6; 200 MHz; 25.0 ºC; TMS).

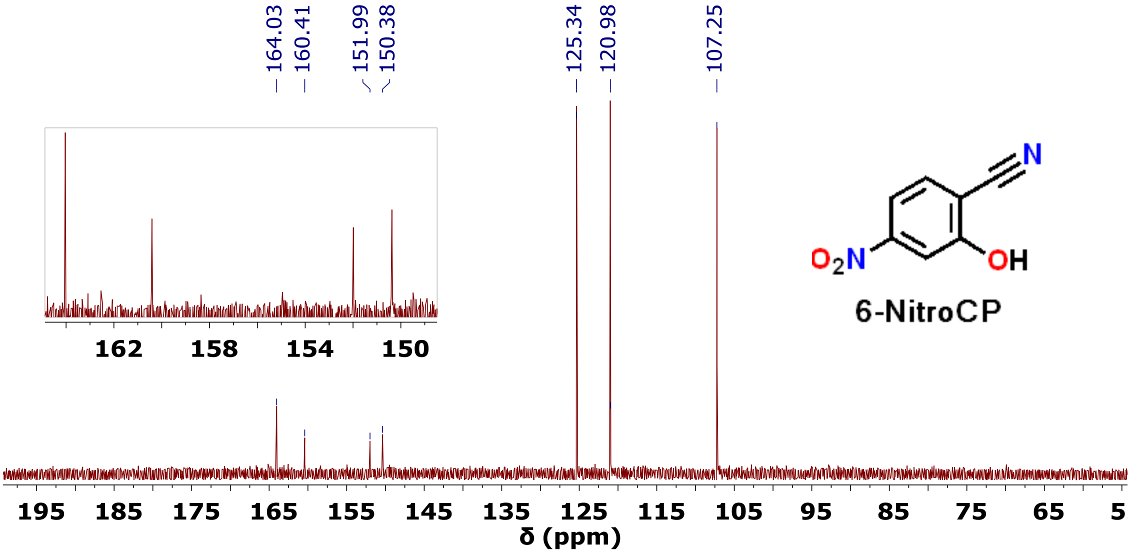

Figure S3-b. ^{13}C{^{1}H} NMR spectra of 6-NitroCP (Acetone-D_6; 50 MHz; 25.0 ºC; Residual solvent as reference).

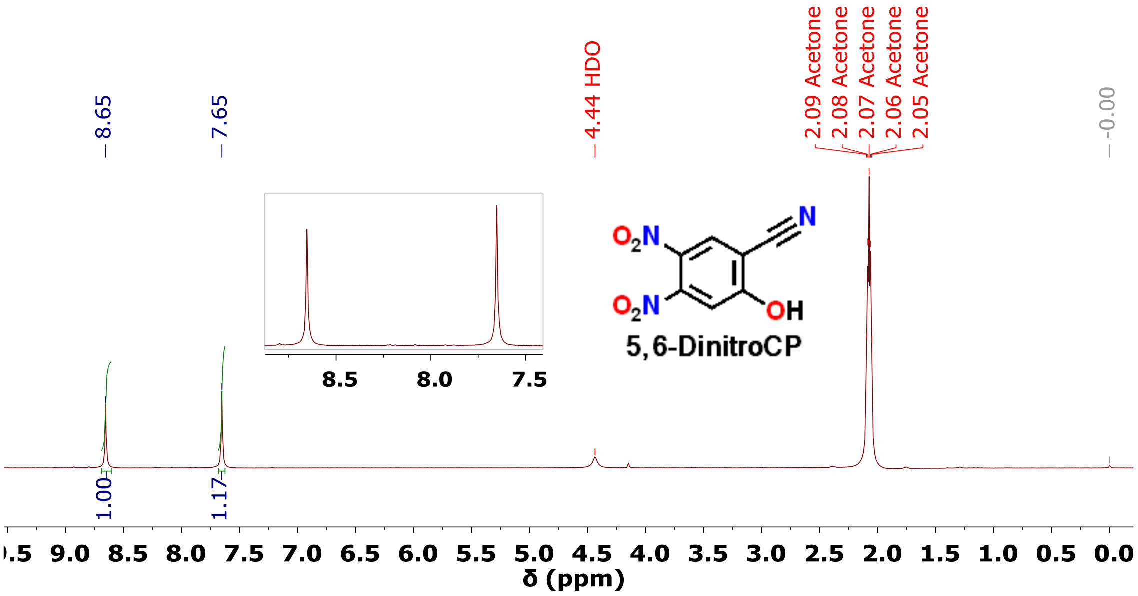

Figure S4-a. ^{1}H NMR spectra of 5,6-DinitroCP (Acetone-D_6; 200 MHz; 25.0 ºC; TMS).

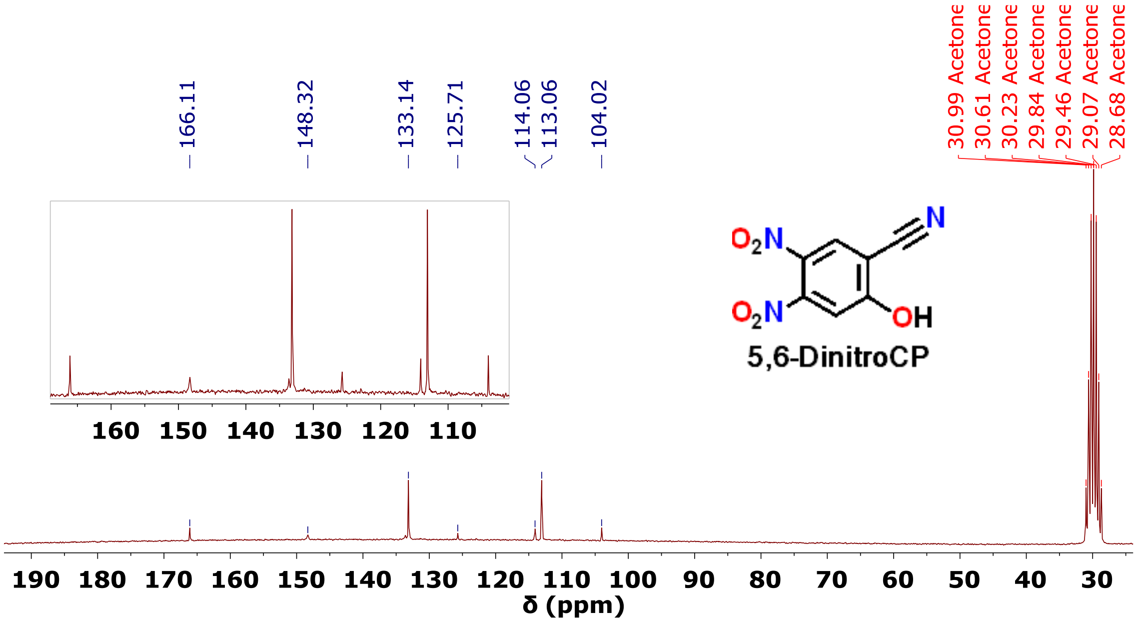

Figure S4-b. $^{13}C\{^1H\}$ NMR spectra of 5,6-DinitroCP (Acetone-D_6; 50 MHz; 25.0 ºC; Residual solvent as reference).

3.2 Molar absorption coefficients (ε)

As a complement, the molar absorption coefficient values were determined for both CBI derivatives and CPs in their anionic form (Table S2).

Table S2. Molar absorption coefficient for anionic CBI derivatives and CPs (pH 7.0; 25.0 ºC).

Compound	**ε ($L\cdot mol^{-1}\cdot cm^{-1}$) // λ**
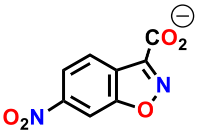 **6-NitroCBI**	8.206,56 // 275 nm
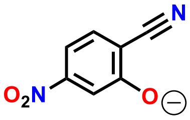 **6-NitroCP**	10.329,02 // 264 nm 2.334,12 // 400 nm
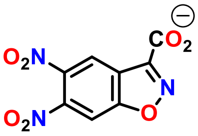 **5,6-DinitroCBI**	10.495,80 // 250 nm
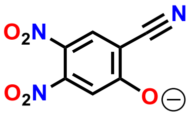 **5,6-DinitroCP**	10.240,31 // 380 nm

4. Kinetic Data

Reactions were followed with an UV-Vis spectrophotometer equipped with Peltier temperature controller set to 25.0 ºC, except to obtain the thermodynamic parameters, which varied between 25-65 ºC.

4.1 Spontaneous decarboxylation reaction in different acetonitrile percentages

The spontaneous decarboxylation reaction of CBIs were investigated at different acetonitrile fractions. The data (Table S3 and Figure S5) show exponential increases in k_{obs} with increasing the acetonitrile percentage (v/v).

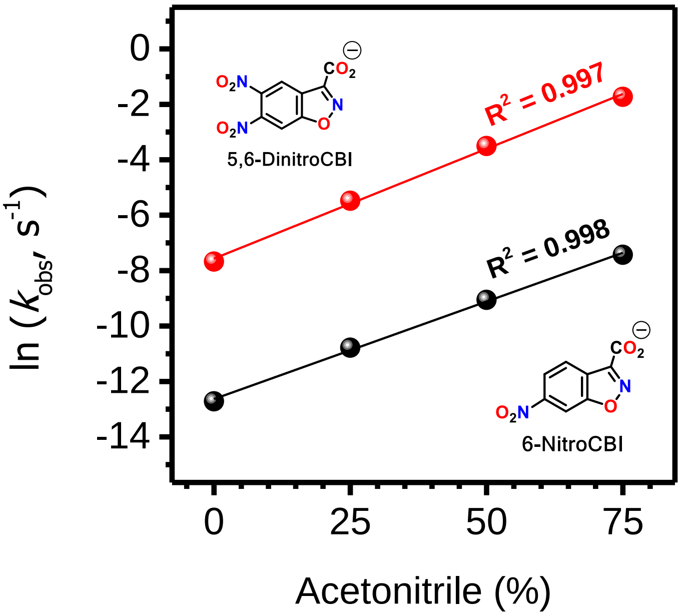

Figure S5. Influence of acetonitrile percentage (v/v) on the k_{obs} for spontaneous decarboxylation reaction of (●) 6-NitroCBI and (●) 5,6-DinitroCBI (pH 7.00; [Bis-Tris methane] = 0.01 mol·L^{-1}; 25.0 ºC).

Table S3. k_{obs} to spontaneous decarboxylation reaction of CBI derivatives in different acetonitrile percentages (pH 7.0; [Bis-Tris methane] = 0.01 mol·L^{-1}; 25.0 ºC).

CH_3CN (%, v/v)	6-NitroCBI (s^{-1})	5,6-DinitroCBI (s^{-1})
0.0	$(3.00 \pm 0.03) \times 10^{-6}$	$(4.65 \pm 0.05) \times 10^{-4}$
25.0	$(2.08 \pm 0.05) \times 10^{-5}$	$(4.18 \pm 0.12) \times 10^{-3}$
50.0	$(1.17 \pm 0.11) \times 10^{-4}$	$(3.01 \pm 0.17) \times 10^{-2}$
75.0	$(5.95 \pm 0.02) \times 10^{-4}$	(0.1775 ± 0.0024)

4.2 pH-rate profiles

The kinetic pK_{a} values (pK_{ac}) for both CBI derivatives were determined by non-linear fitting curves in the pH-rate profile using the Equation S1, the 1.61 and 1.18 values being obtained for 6-NitroCBI and 5,6-DinitroCBI, respectively. Additionally, the increasing in k_{obs} with pH (Figure S6) indicates the anionic species as the most reactive.

$$k_{obs} = k_{\mathrm{HA}}\left(\frac{1}{1+10^{(pH-pKa)}}\right) + k_{\mathrm{A-}}\left(\frac{1}{1+10^{(pKa-pH)}}\right) \qquad \text{(S1)}$$

k_{obs} is the observed rate constant at experimental pH; k_{HA} is the rate constant of the neutral species; $k_{\mathrm{A-}}$ is rate constant of the anionic species.

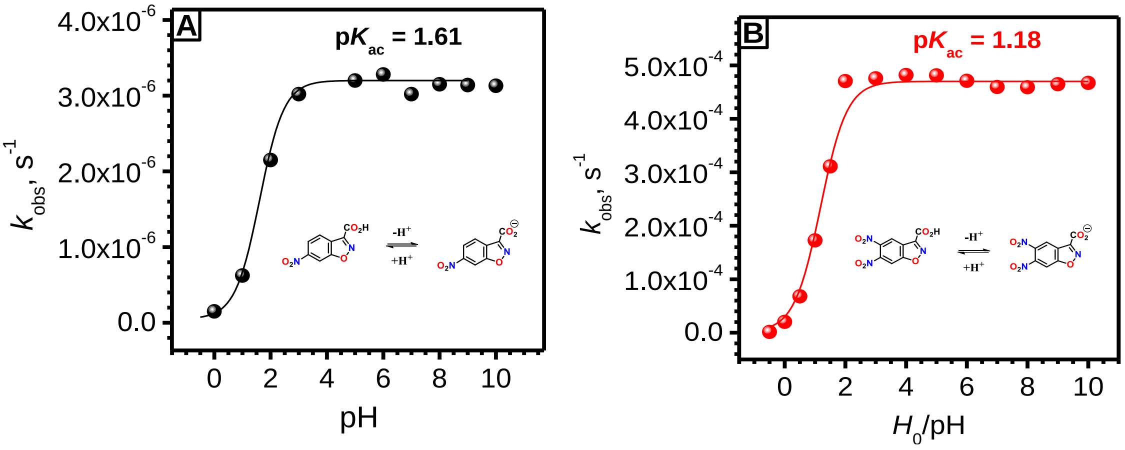

Figure S6. pH-rate profile to spontaneous decarboxylation reaction of 6-NitroCBI (**A**) and 5,6-DinitroCBI (**B**) ([CBIs] = 1.0 × 10^{-4} mol·L^{-1}; 25.0 ºC).

4.3 Activation parameters

The spontaneous decarboxylation reaction of anionic CBI derivatives was investigated at different temperatures to determine the activation parameters by Eyring relationship. Table S4 shows the values of k_{obs} as a function of temperature, with good linear relationship in the Eyring plot (Figure S7).

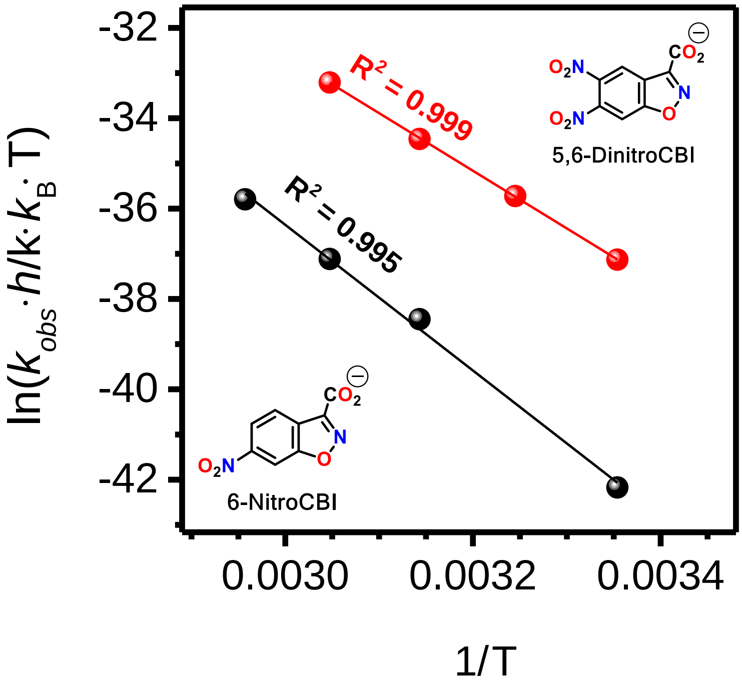

Figure S7. Eyring plot to spontaneous decarboxylation reaction of (●) 6-NitroCBI and (●) 5,6-DinitroCBI (pH 7.00; [Bis-Tris methane] = 0.01 mol·L^{-1}).

Table S4. k_{obs} to spontaneous decarboxylation reaction of anionic CBI derivatives between 25-65 ºC (pH 7.0; [Bis-Tris methane] = 0.01 M).

T (ºC)	**6-NitroCBI (s^{-1})**	**5,6-DinitroCBI (s^{-1})**
25.0	$(3.00 \pm 0.0) \times 10^{-6}$	$(4.65 \pm 0.0) \times 10^{-4}$
35.0	---	$(1.96 \pm 0.0) \times 10^{-3}$
45.0	$(1.33 \pm 0.0) \times 10^{-4}$	$(7.18 \pm 0.1) \times 10^{-3}$
55.0	$(5.20 \pm 0.1) \times 10^{-4}$	$(2.59 \pm 0.2) \times 10^{-2}$
65.0	$(2.01 \pm 0.3) \times 10^{-3}$	---

4.4 Influence of TMA concentration

The decarboxylation reactions were investigated in the presence of different tetramethylammonium bromide (TMA) concentrations in order to simulate the high concentration of NMe_3^+ groups found in the pillararene portals. The exponential increments on k_{obs} (Figure S8) observed for 6-NitroCBI⊂P6A, 5,6-DinitroCBI⊂P5A and 5,6-DinitroCBI⊂P6A systems equate to spontaneous decarboxylation of the corresponding derivative at TMA concentrations of 2.02, 2.85 and 3.80 mol·L^{-1}, respectively.

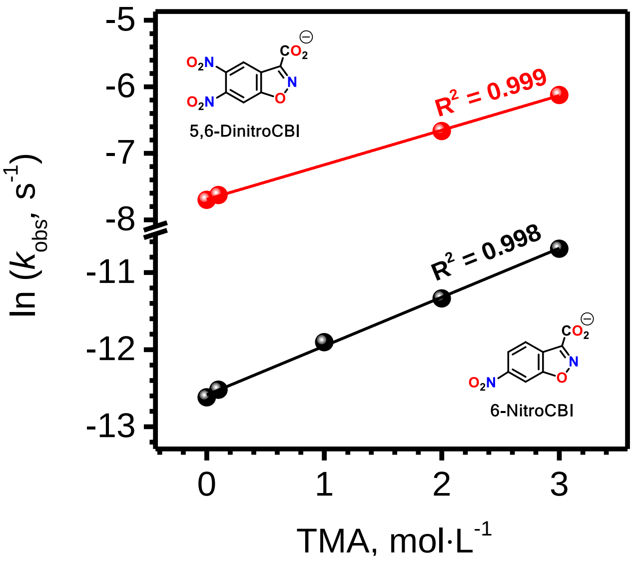

Figure S8. Influence of TMA concentration on k_{obs} for decarboxylation reaction of (●) 6-NitroCBI and (●) 5,6-DinitroCBI in aqueous media ([CBIs] = 1.0 × 10^{-4} mol·L^{-1}; pH 7.00; [Bis-Tris methane] = 0.01 mol·L^{-1}; 25.0 °C).

4.5 Determination of the constants

The experiments of k_{obs} *vs.* [Pillararene] showed catalytic or inhibitory effects on CBIs decarboxilation, reaching a plateau. This effect can be explained by the host-guest complexation of CBI derivatives in the pillararene cavity, with the reaction occurring in both environments (H_2O and pillararenes cavity). Therefore, the k_{obs} is the sum of the rate constants in both environments weighted by their molar fractions. To assessment the stoichiometry we consider the H:G (Equation S2) and H:G_2 (Equation S3) models for fitting data, however, for H:G_2 errors up to 400 and 900 % were observed on the rate ($k_{1:1}$ and $k_{1:2}$) and binding ($K_{1:1}$ and $K_{1:2}$) constants, respectively. Thus, these parameters were determined considering only the formation of low order complexes (H:G), this stoichiometry being confirmed for some systems by ^{1}H NMR titration.

H:G stoichiometry

$$k_{obs} = k_w X_w + k_{1:1} X_{1:1} \qquad \text{(S2)}$$

$$X_w = \frac{1}{1+K_{1:1}[Pillar]} \qquad X_{1:1} = \frac{K_{1:1}[Pillar]}{1+K_{1:1}[Pillar]}$$

k_w and $k_{1:1}$ are the rate constants in H_2O and pillararene cavity, respectively; X_w and $X_{1:1}$ are the molar fractions of CBI derivative in H_2O and pillararene cavity, respectively.

H:G$_2$ stoichimetry

$$k_{obs} = k_w X_w + k_{1:1} X_{1:1} + k_{1:2} X_{1:2} \tag{S3}$$

$$X_w = \frac{1}{1+K_{1:1}[Pillar]+K_{1:1}K_{1:2}[Pillar]^2}$$

$$X_{1:1} = \frac{K_{1:1}[Pillar]}{1+K_{1:1}[Pillar]+K_{1:1}K_{1:2}[Pillar]^2}$$

$$X_{1:2} = \frac{K_{1:1}K_{1:2}[Pillar]^2}{1+K_{1:1}[Pillar]+K_{1:1}K_{1:2}[Pillar]^2}$$

$k_{1:1}$ and $k_{1:2}$ are the rate constants in the systems H:G and H:G$_2$, respectively; $X_{1:1}$ and $X_{1:2}$ are the molar fractions of the H:G and H:G$_2$ complexes, respectively; $K_{1:1}$ and $K_{1:2}$ are the association constants of formation of the H:G and H:G$_2$ complexes, respectively.

5. NMR experiments

5.1 ^{1}H NMR titration

All NMR analyses were performed using a Bruker AC 200 MHz spectrometer. The fast decarboxylation of 5,6-DinitroCBI (even faster in the presence of organic solvent) made its titration impossible. Thus, the successive spectra presented below correspond only to experiments involving 6-NitroCBI and both pillararenes (P5A and P6A). The successive spectra of Figure S9 shows the chemical shifts of aromatic protons of the 6-NitroCBI and pillararenes as a function of the 6-NitroCBI:Pillararene molar ratio.

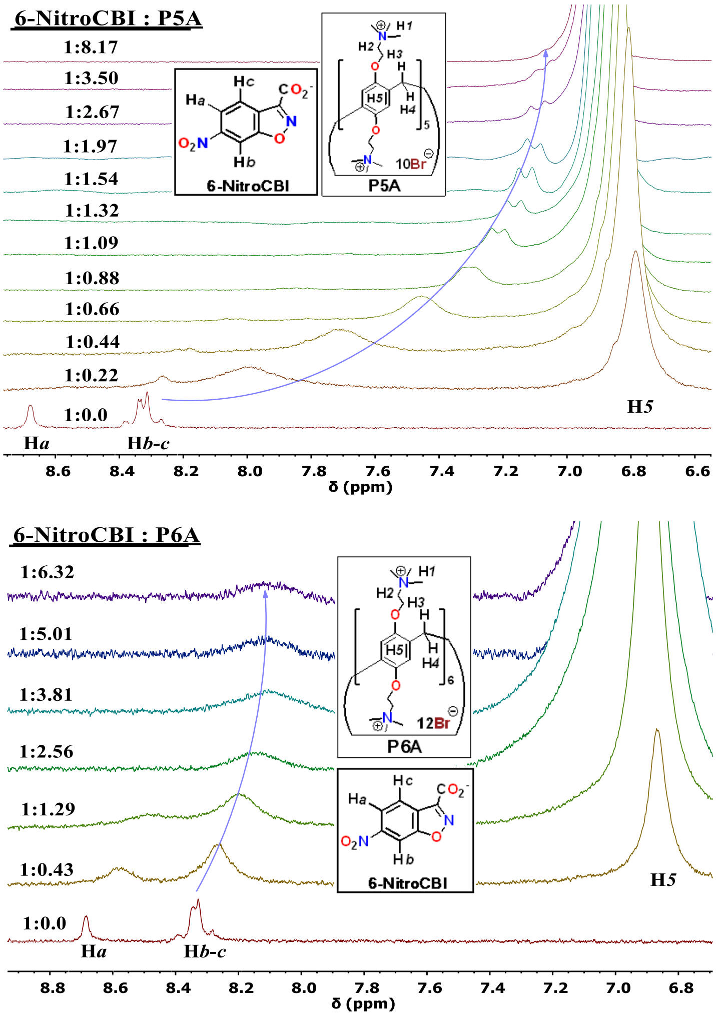

Figure S9. Chemical shifts of the 6-NitroCBI (**UP** = 12.93 mM; **BOTTOM** =7.65 mM) and pillararenes aromatic protons as a function of P5A (**UP**) and P6A (**BOTTOM**) equivalents (D_2O:MeOD, 8:2, v/v; 25.0 °C; 200 MHz).

The successive spectra of Figure S10 shows the representative chemical shifts of the aliphatic protons of pillararenes for the same experiment as in Figure S9. These spectra show in more details one of the factors responsible for inhibitory effect in the 6-NitroCBI⊂P5A system: reduction of inductive effect of NO_2 group by field effects (described in the manuscript).

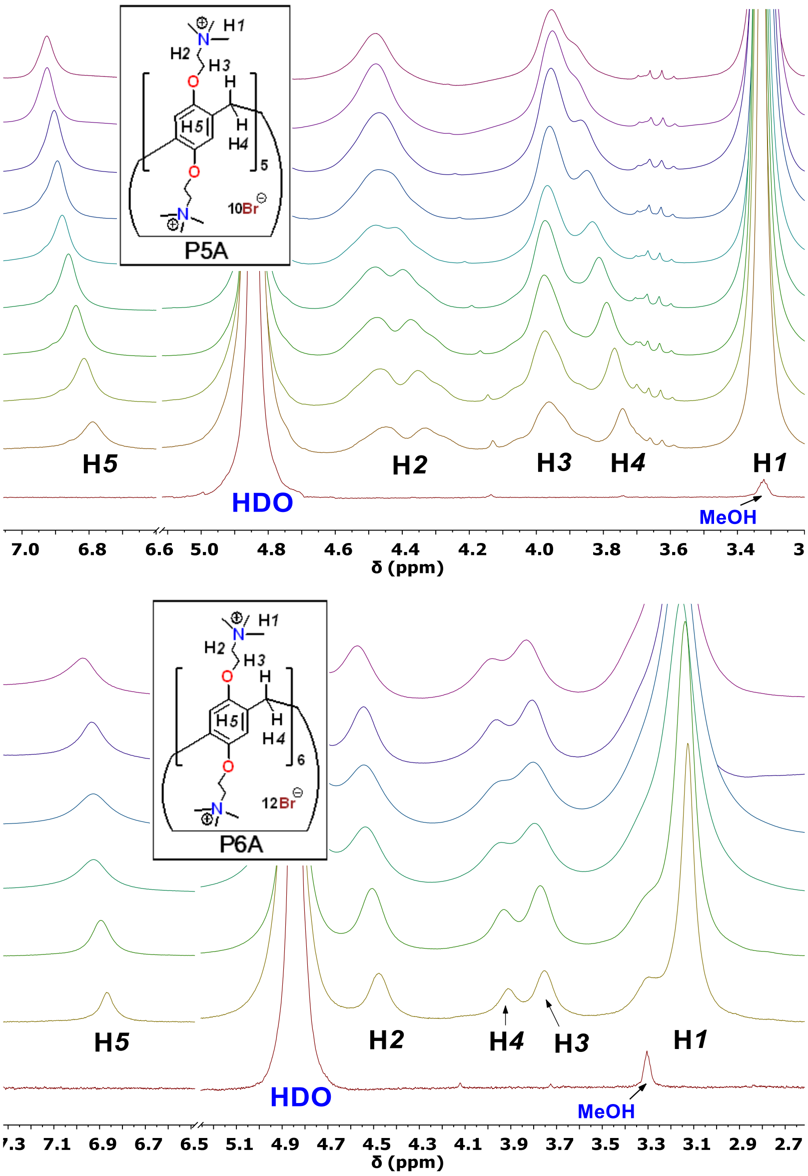

Figure S10. Representative chemical shifts of the pillararenes aliphatic protons as a function of 6-NitroCBI:Pillararene molar ratio for P5A (**UP**) and P6A (**BOTTOM**) (D_2O:MeOD, 8:2, v/v; 25.0 °C; 200 MHz).

5.2 Treatment of the NMR data

The graphics of Δδ *vs*. [Pillararene]$_0$ were fitted to investigate the stoichiometry and magnitude of the association constant. For this, we use the H:G model described below.[3]

H:G stoichiometry

Assuming only the existence of the H:G complex (H + G $\rightleftharpoons$ H:G), the binding constant is defined by:

$$K_{1:1} = \frac{[\mathrm{H{:}G}]}{[\mathrm{H}]\cdot[\mathrm{G}]}$$

Due to the free concentrations cannot be measured directly, an alternative approach to use [Pillararene]$_0$ and [6-NitroCBI]$_0$ can be solved, reaching:

$$[\mathrm{H{:}G}] = \frac{1}{2}\left\{[\mathrm{Pillar}]_0 + [\mathrm{CBI}]_0 + \frac{1}{K_{1:1}} - \sqrt{\left([\mathrm{Pillar}]_0 + [\mathrm{CBI}]_0 + \frac{1}{K_{1:1}}\right)^2 - 4[\mathrm{Pillar}]_0[\mathrm{CBI}]_0}\right\}$$

Lastly, the experimental data was fitted with the Equation S4:

$$\Delta\delta = \delta_{1:1}\left(\frac{[\mathrm{H{:}G}]}{[\mathrm{H}]_0}\right) \qquad \text{(S4)}$$

6. Theoretical Study

6.1 Intrinsic reaction coordinates and transition states

The intrinsic reaction coordinates (IRCs) and transition states to spontaneous decarboxylation reaction of the 6-NitroCBI and 5,6-DinitroCBI are presented bellow.

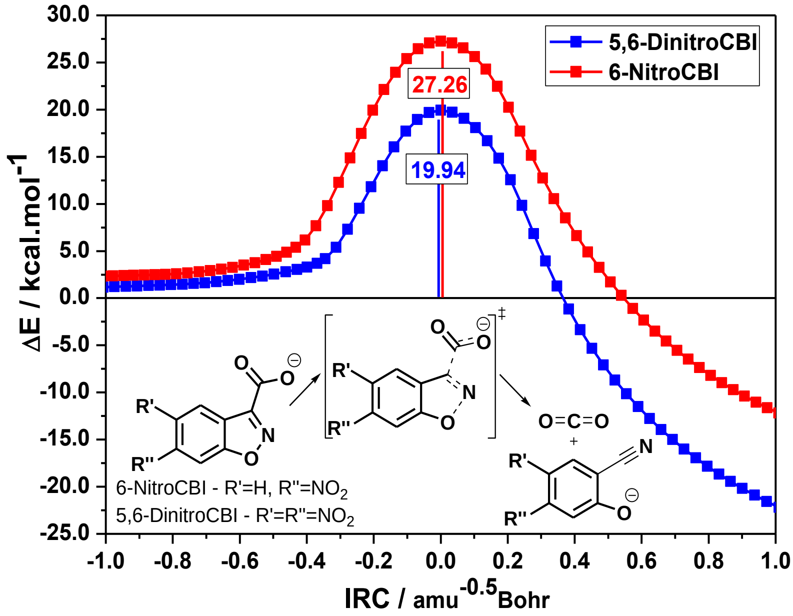

Figure S11-a. Intrinsic reaction coordinates to decarboxylation reaction of (🟥) 6-NitroCBI and (🟦) 5,6-DinitroCBI (M06/6-31G+(d,p) theory level).

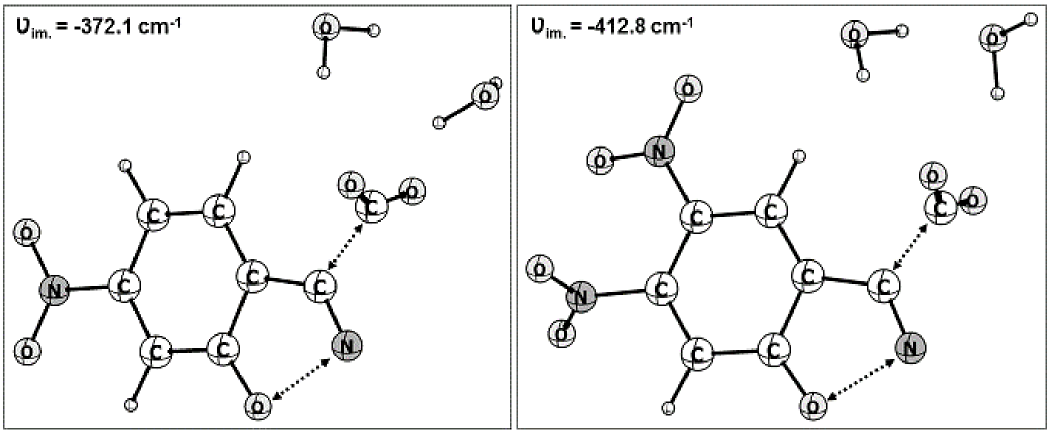

Figure S11-b. Transition states to decarboxylation reaction of (left) 6-NitroCBI and (right) 5,6-DinitroCBI (M06/6-31G+(d,p) theory level).

6.2 Cartesian coordinates at the PCM M06/6-31+G(d,p) level

6-NitroCBI - Global minimum + 2 H_2O (HF = -944.7557989 Hartrees)

C	2.108987	-1.403861	-0.052001
H	2.547921	-2.394977	-0.079268
C	2.945321	-0.275861	-0.005485
C	2.490672	1.033255	0.032222
H	3.155975	1.888580	0.067477
C	1.111173	1.148949	0.018960
C	0.235185	0.066369	-0.027912
C	0.737508	-1.240715	-0.064087
H	0.075103	-2.099190	-0.098674
N	4.392756	-0.489559	0.005382
O	4.811187	-1.640585	-0.028776
O	5.125030	0.492359	0.047362
C	-1.056572	0.690229	-0.022139
C	-2.408524	0.024091	-0.063666
O	0.403960	2.308612	0.047217
O	-3.424875	0.766318	0.045380
O	-2.401036	-1.218221	-0.199844
N	-0.949490	1.992672	0.022536
H	-4.543501	-0.225047	1.198616
H	-4.722775	-0.046736	-1.024718
H	-4.995465	-1.674939	1.385897
H	-5.272712	-1.435556	-1.363886
O	-5.367782	-0.504828	-1.601313
O	-5.062723	-0.802237	1.792948

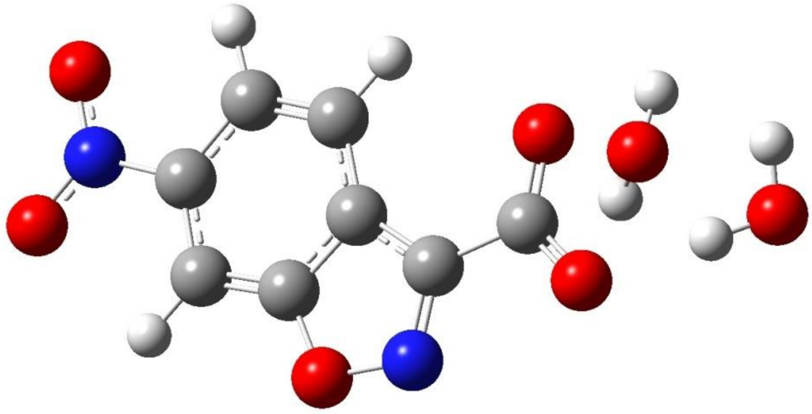

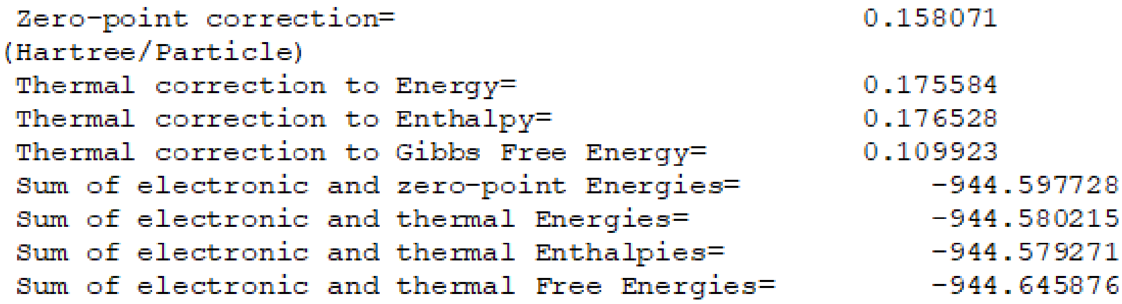

```
 Zero-point correction=                           0.158071
(Hartree/Particle)
 Thermal correction to Energy=                    0.175584
 Thermal correction to Enthalpy=                  0.176528
 Thermal correction to Gibbs Free Energy=         0.109923
 Sum of electronic and zero-point Energies=           -944.597728
 Sum of electronic and thermal Energies=              -944.580215
 Sum of electronic and thermal Enthalpies=            -944.579271
 Sum of electronic and thermal Free Energies=         -944.645876
```

6-NitroCBI - TS + 2 H_2O (HF = -944.712377 Hartrees)

C	-1.672786	-1.294823	0.112576
H	-1.882702	-2.355837	0.176528
C	-2.710936	-0.360790	0.007835
C	-2.539574	1.007101	-0.081245
H	-3.386742	1.679941	-0.158879
C	-1.222510	1.528396	-0.069430
C	-0.164878	0.564332	0.038180
C	-0.378540	-0.810324	0.126129
H	0.463522	-1.494595	0.203179
N	-4.087853	-0.871097	-0.012864
O	-4.262048	-2.078682	0.104208
O	-5.006591	-0.071601	-0.147108
C	1.069147	1.297500	0.032414
C	2.576834	0.395365	0.189811
O	-0.933150	2.773232	-0.148975
O	2.972401	0.099901	-0.921374
O	2.819684	0.243416	1.363181
N	1.198240	2.510060	-0.053237
H	3.203332	-1.995921	-0.777370
H	4.953167	-0.237021	-0.605165
H	3.739937	-2.536604	0.541458
H	5.611158	-0.673098	0.701938
O	5.821097	-0.374539	-0.192188
O	3.311743	-2.819248	-0.277318

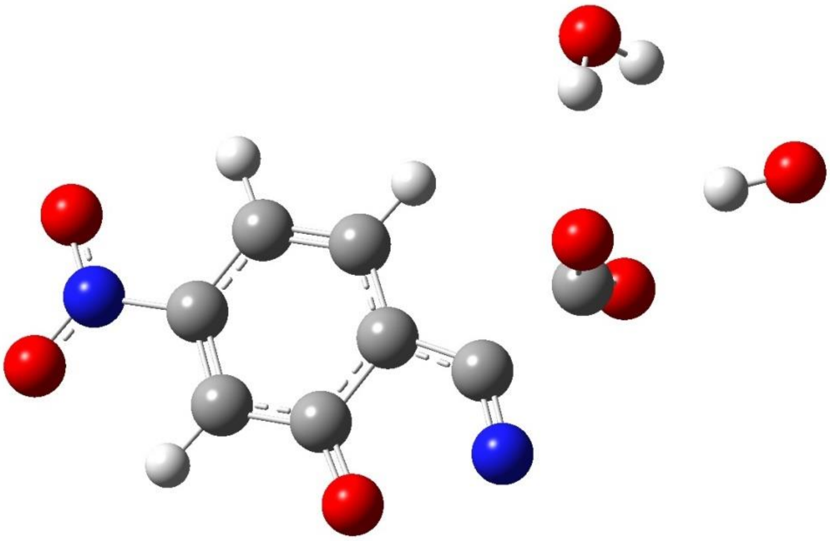

```
 Zero-point correction=                           0.153991
(Hartree/Particle)
 Thermal correction to Energy=                    0.172264
 Thermal correction to Enthalpy=                  0.173209
 Thermal correction to Gibbs Free Energy=         0.105980
 Sum of electronic and zero-point Energies=          -944.558386
 Sum of electronic and thermal Energies=             -944.540113
 Sum of electronic and thermal Enthalpies=           -944.539168
 Sum of electronic and thermal Free Energies=        -944.606397
```

5,6-DinitroCBI - Global minimum + 2 H_2O (HF = -1149.1596139 Hartrees)

C	1.794544	0.723595	-0.008621
C	2.514700	-0.492719	0.006631
C	1.889995	-1.717505	0.031519
H	2.448938	-2.647882	0.015998
C	0.498455	-1.666997	0.021873
C	-0.238422	-0.488315	-0.018884
C	0.414585	0.744949	-0.025398
H	-0.125905	1.685647	-0.000620
N	3.975931	-0.519977	-0.142494
O	4.459615	0.136909	-1.050094
O	4.602443	-1.239957	0.616367
C	-1.596936	-0.946812	-0.018957
C	-2.855478	-0.115234	-0.065434
O	-0.332595	-2.725926	0.036391
O	-3.952057	-0.729515	0.043271
O	-2.686249	1.113721	-0.206041
N	-1.647686	-2.250867	0.011577
H	-5.162174	0.206735	-1.041973
H	-4.985473	0.355592	1.187004
H	-5.632272	1.645458	-1.270942
H	-5.547000	1.778444	1.279424
O	-5.479079	0.955804	1.779950
O	-5.745535	0.748818	-1.610177
N	2.480506	2.000919	0.137832
O	1.954104	2.991715	-0.346211
O	3.531098	2.013395	0.767335

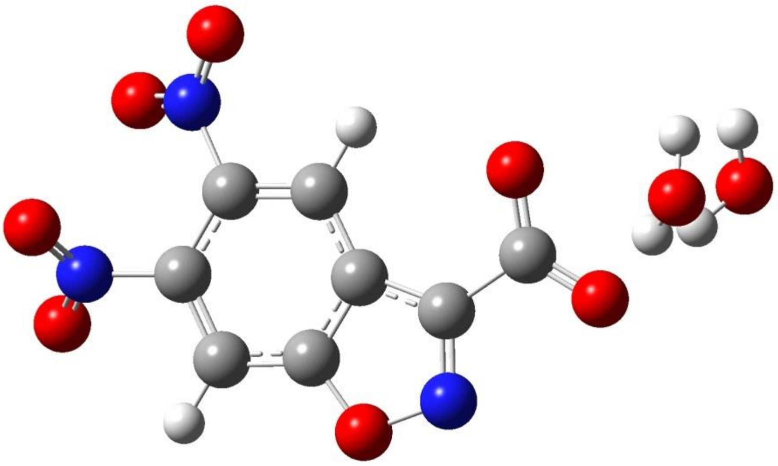

```
 Zero-point correction=                           0.159854
(Hartree/Particle)
 Thermal correction to Energy=                    0.180271
 Thermal correction to Enthalpy=                  0.181215
 Thermal correction to Gibbs Free Energy=         0.108365
 Sum of electronic and zero-point Energies=          -1148.999760
 Sum of electronic and thermal Energies=             -1148.979343
 Sum of electronic and thermal Enthalpies=           -1148.978399
 Sum of electronic and thermal Free Energies=        -1149.051248
```

5,6-DinitroCBI - TS + 2 H_2O (HF = -1149.1278348 Hartrees)

C	1.258659	-0.640749	-0.042254
C	2.265464	0.351961	-0.048414
C	2.000689	1.692655	-0.048679
H	2.803753	2.423777	-0.032279
C	0.642568	2.122812	-0.021041
C	-0.363210	1.097182	0.013231
C	-0.075655	-0.250492	-0.005559
H	-0.863396	-1.002758	-0.017598
N	3.693642	-0.005576	0.060170
O	4.064394	-0.487286	1.116277
O	4.411764	0.259890	-0.887006
C	-1.634871	1.767336	0.047173
C	-3.068934	0.822712	0.100224
O	0.266393	3.333765	-0.013983
O	-3.470532	0.625573	-1.032233
O	-3.310985	0.517508	1.251063
N	-1.760993	2.991137	0.051389
H	-4.483341	-1.040559	-1.058027
H	-3.405272	-2.374910	0.330814
H	-5.578084	-1.929132	-0.441497
H	-2.682867	-1.593400	1.428784
O	-2.681585	-2.453551	0.985378
O	-4.733820	-1.969911	-0.908409
N	1.569799	-2.030117	-0.174794
O	0.683192	-2.855408	0.034455
O	2.714155	-2.339533	-0.512498

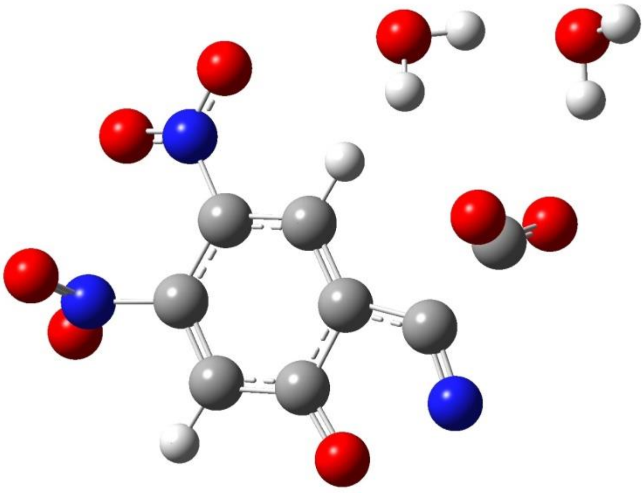

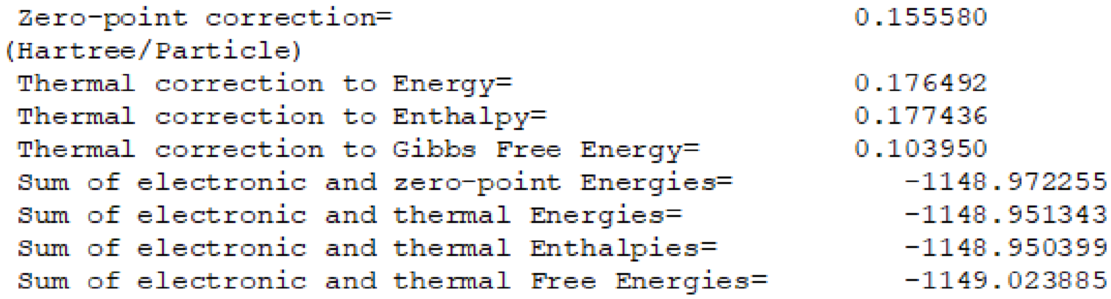

```
 Zero-point correction=                           0.155580
(Hartree/Particle)
 Thermal correction to Energy=                    0.176492
 Thermal correction to Enthalpy=                  0.177436
 Thermal correction to Gibbs Free Energy=         0.103950
 Sum of electronic and zero-point Energies=          -1148.972255
 Sum of electronic and thermal Energies=             -1148.951343
 Sum of electronic and thermal Enthalpies=           -1148.950399
 Sum of electronic and thermal Free Energies=        -1149.023885
```

6.3 Molecular dynamics simulations

As described in the manuscript, the five parameters (P1-P5) assessment to the four geometric structures of the complexes were: (P1) the average distance between carbon 6 (C6) from CBI derivative and the center of the pillararene cavity (CPC); (P2) the spatial orientation/angle of the CBI derivative in the CPC; (P3) the average distance between charged groups (COO^- and NMe_3^+); (P4) the energetic contributions resulting from electrostatic (EL) and Van der Waals (VDW) interactions and (P5) the number of HBs between water and COO^- group from CBI derivative. All of these parameters were well discussed in the manuscript and their corresponding graphs are shown below (Figures S12-S16).

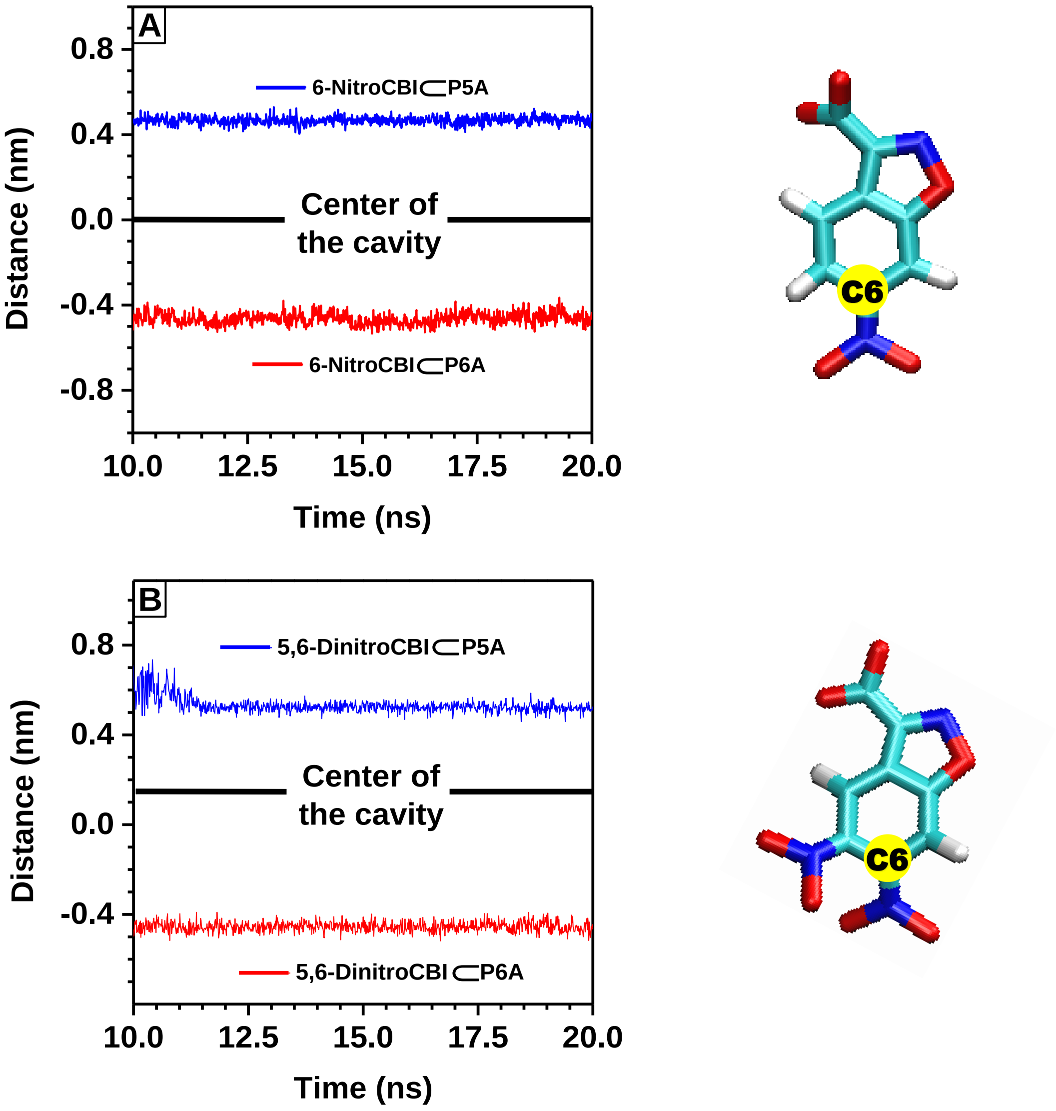

Figure S12. Calculated distances between the center of the pillararenes cavity (▬, P5A; ▬, P6A) and C6 carbon from 6-NitroCBI (**A**) and 5,6-DinitroCBI (**B**), as a function of the simulation time.

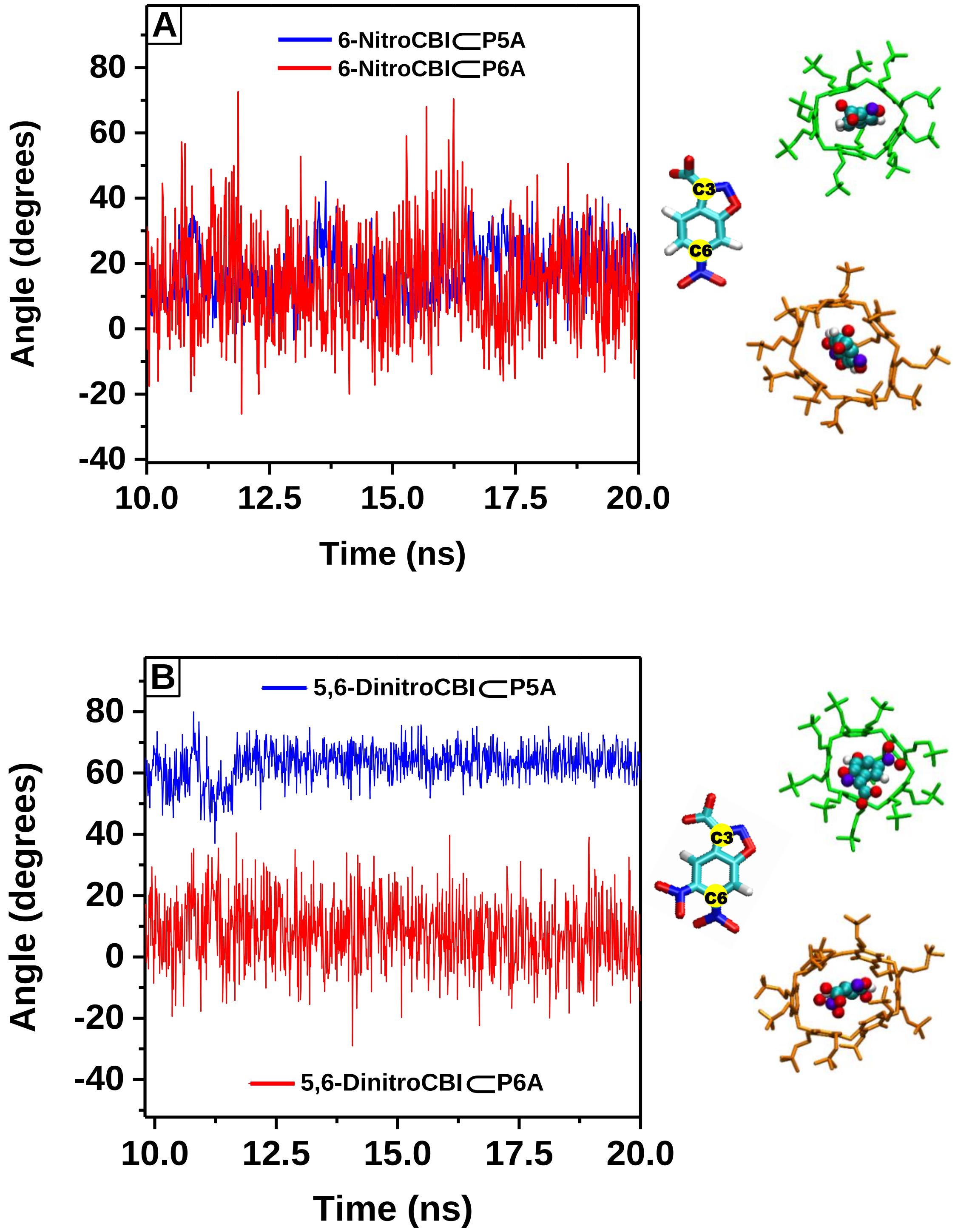

Figure S13. Angles between V1 (center of the pillararenes cavity) and V2 (C3 and C6 carbons of the CBIs) longitudinal vectors for 6-NitroCBI (**A**) and 5,6-DinitroCBI (**B**) complexed with P5A (▬) and P6A (▬), as a function of time. On the right side of the graphs are the simulated structures for the complexes, seen from the top.

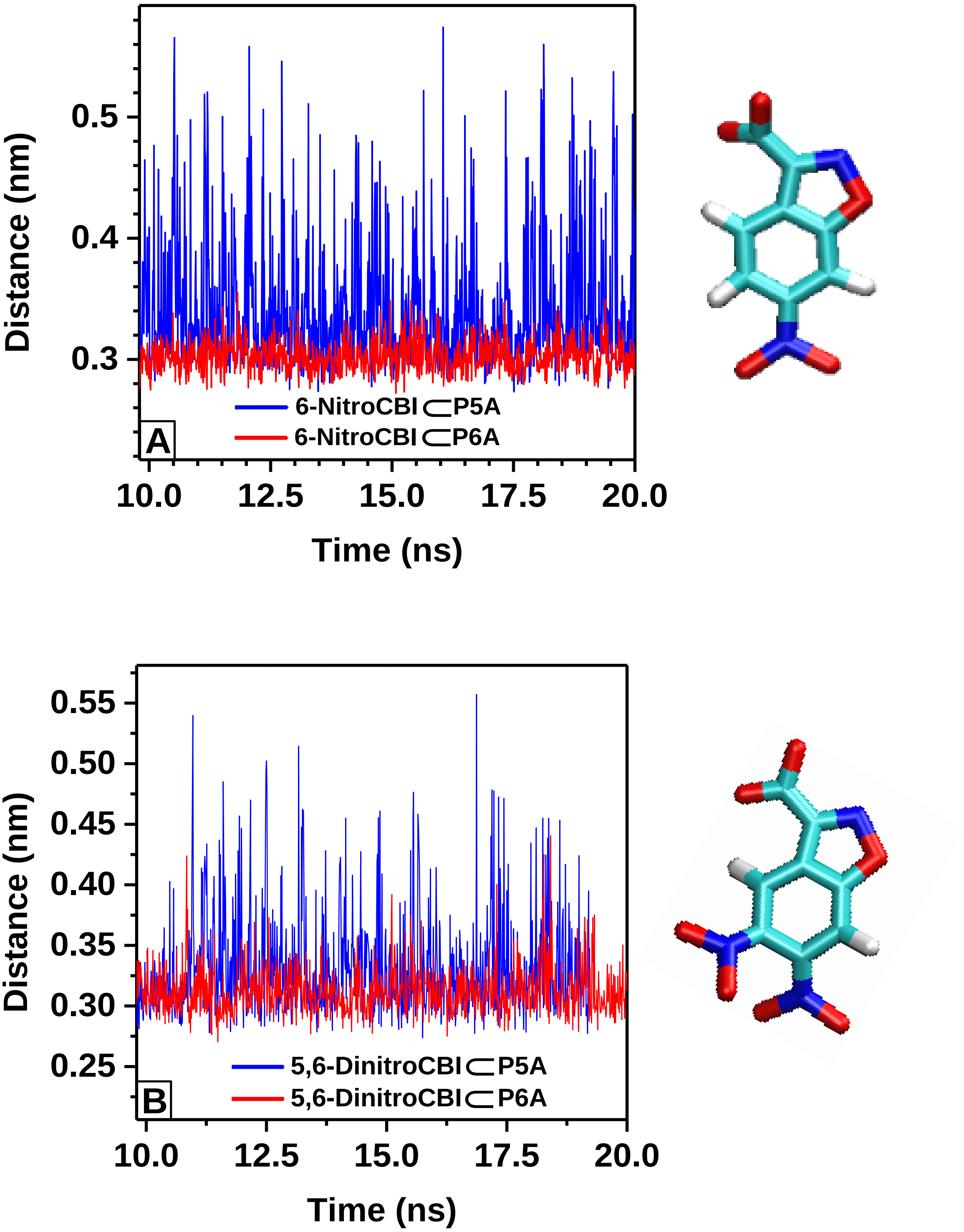

Figure S14. Distance between NMe$_3^+$ groups from pillararenes (—, P5A; —, P6A) and COO$^-$ groups from 6-NitroCBI (**A**) and 5,6-DinitroCBI (**B**).

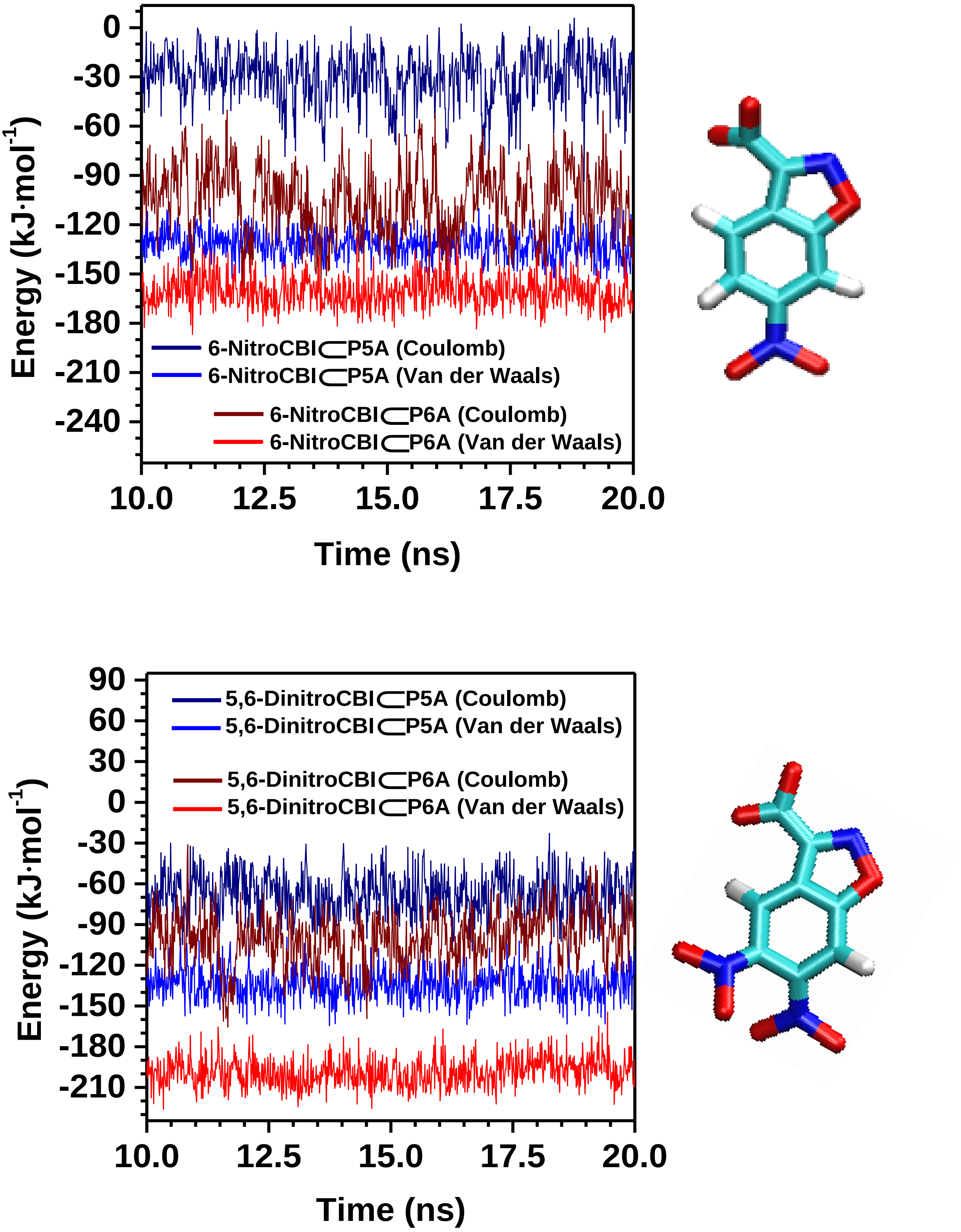

Figure S15. Energy minimization promoted by electrostatic (Coulomb potential) and Van der Waals (Lennard-Jones potential) interactions between pillararenes (P5A, blue color; P6A, red color) and 6-NitroCBI (**Above**) or 5,6-DinitroCBI (**Below**).

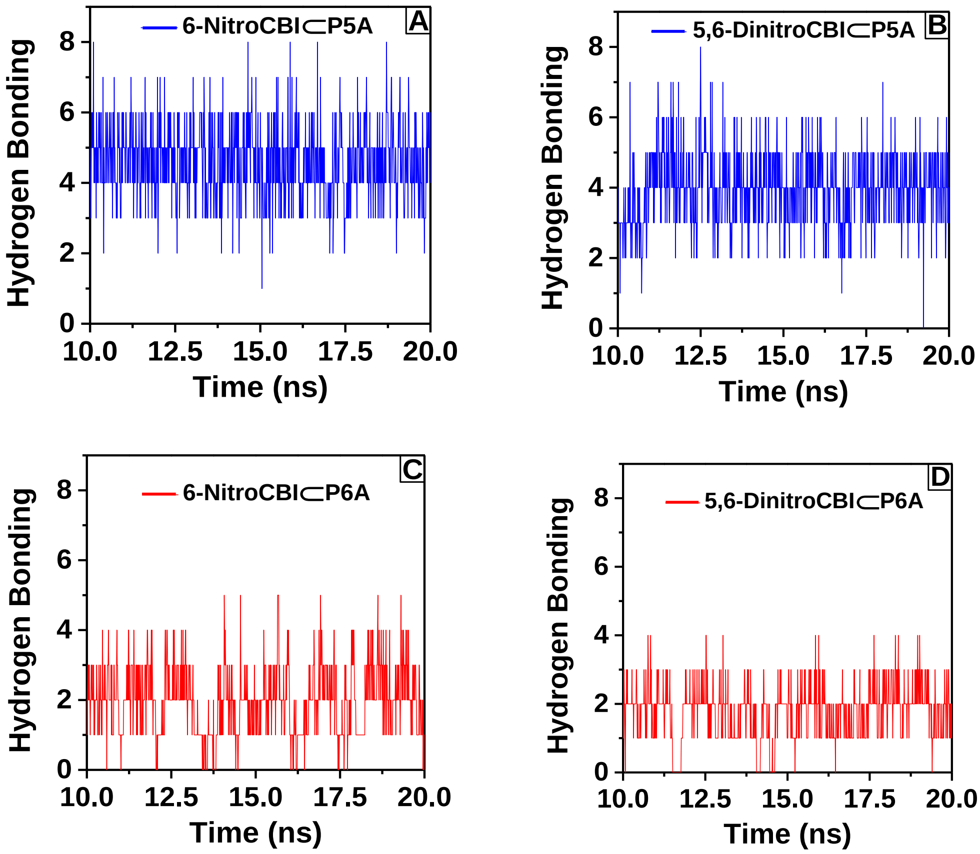

Figure S16. Number of hydrogen bonds between water and COO^- group (from CBI derivatives) for 6-NitroCBI⊂P5A (**A**), 5,6-DinitroCBI⊂P5A (**B**), 6-NitroCBI⊂P6A (**C**) and 5,6-DinitroCBI⊂P6A (**D**) complexes, as a function of time.

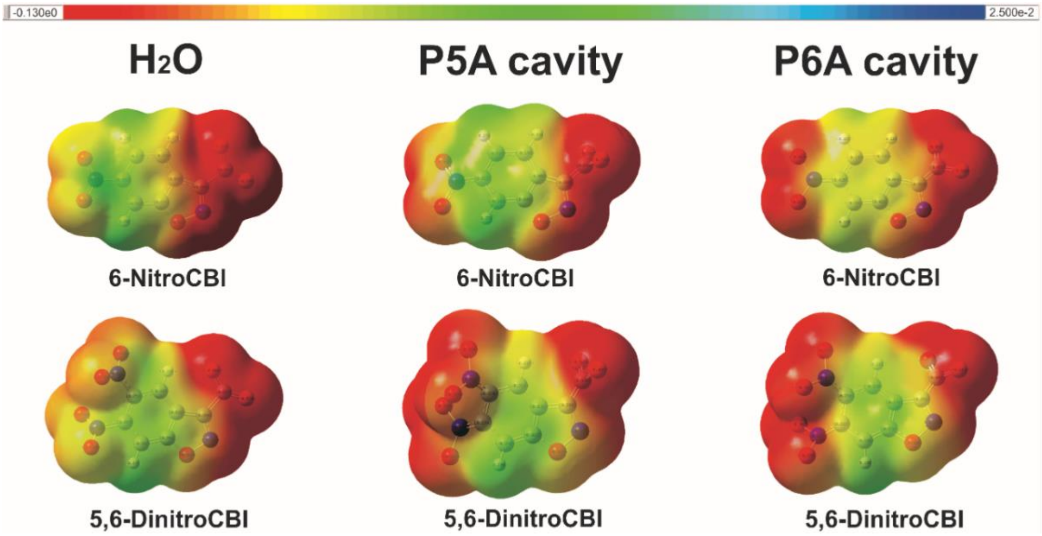

Figure S17. 3D-representation of the electrostatic potentials (ELP) around the CBI nitrated derivatives in water (PCM) and in the geometric structure of the four complexes (DFT/B3LYP level of theory at 6-31G*).

7. References

1. D. S. Kemp, K. G. Paul, *J. Am. Chem. Soc.*, 1975, **97**,7305–7312.
2. E. V. Silveira, V. Nascimento, E. H. Wanderlind, R. F. Affeldt, G. A. Micke, L. Garcia-Rio, F. Nome, *J. Org. Chem.*, 2019, **84**, 9684–9692.
3. P. Thordarson, *Chem. Soc. Rev.*, 2011, **40**, 1305–1323.